Selective generation of local ferromagnetism in austenitic stainless steel using nanoindentation

J. Sort, A. Concustell, E. Menéndez, S. Suriñach, M. D. Baró, J. Farran, and J. Nogués

Selective generation of local ferromagnetism in austenitic stainless steel using nanoindentation

J. Sort[a)]
Institució Catalana de Recerca i Estudis Avançats (ICREA) and Departament de Física,
Universitat Autònoma de Barcelona, Bellaterra, Barcelona 08193, Spain

A. Concustell, E. Menéndez, S. Suriñach, and M. D. Baró
Departament de Física, Universitat Autònoma de Barcelona, Bellaterra, Barcelona 08193, Spain

J. Farran
Suñer S.A., Balmes 73, Sabadell 08203, Spain

J. Nogués
Institució Catalana de Recerca i Estudis Avançats (ICREA) and Departament de Física,
Universitat Autònoma de Barcelona, Bellaterra, Barcelona 08193, Spain

Periodic arrays of magnetic structures with micrometrer and submicrometer lateral sizes have been prepared at the surface of an austenitic stainless steel by means of local deformation using a nanoindenter. This method takes advantage of the phase transformation (from nonmagnetic fcc austenite to ferromagnetic bct martensite) which occurs in this material upon plastic deformation. The local character of the induced ferromagnetism is confirmed by magneto-optical Kerr effect measurements together with magnetic force microscopy imaging. The generated ferromagnetism can be subsequently erased by subjecting the deformed steel to annealing processes at temperatures above the reverse, martensite-to-austenite, phase transformation temperature. © *2006 American Institute of Physics*. [DOI: 10.1063/1.2227827]

Austenitic stainless steels are extensively used in widespread industrial and technological applications due to their good corrosion resistance combined with their relatively high strength, toughness, and stiffness.[1,2] In particular, stainless steel is employed as structural material to manufacture turbine blades or bridges and also in nuclear power plants to construct pipes through which pressurized water flows at high temperature. It is well known that when stress is applied to austenitic stainless steel, a phase transformation from the face-centered cubic austenite to a body-centered tetragonal martensite phase occurs.[3,4] The control of this transformation is of crucial importance for the safe operation of steel-based applications. Namely, the appearance of martensite can increase the overall mechanical hardness but sometimes this is accompanied with the formation of cracks.[5,6]

At room temperature, the austenite phase is paramagnetic, while it becomes antiferromagnetic below its Néel temperature, which is about 40 K.[7] Conversely, the stress-induced martensite phase is ferromagnetic, as it has been demonstrated by a number of different techniques.[8–12] Actually, these properties are being exploited to develop novel nondestructive methods, using magnetic measurements, to evaluate the degradation of austenitic steel.[13–15] However, in some cases, the formation of martensite is desirable. For example, subjecting austenitic stainless steel to mechanical attrition treatments leads to the formation of a continuous nanocrystalline surface of martensite phase, which can result in improved mechanical hardness. Magnetic measurements (e.g., Mössbauer spectroscopy) are used also in this case to explore the microstructure evolution during the surface treatment.[16]

Hence, the majority of studies involving magnetic measurements in austenitic stainless steel are aimed at the detection of martensite, which in general is generated from austenite over large and/or uncontrolled areas. In this work, we use the stress-induced martensitic transformation to selectively generate, by means of nanoindentation, arrays of ferromagnetic structures, with micrometer and submicrometer sizes (at least in one of the lateral dimensions) at the surface of a nonmagnetic austenitic stainless steel. It should be noted that conventional methods for the fabrication of magnetic dots, such as electron beam lithography, nanoimprint onto capping resist layers, use of nanotemplates or shadow masks, chemical routes, scanning probe lithography, or irradiation damage are rather complex and typically involve multiple processing steps.[17] Conversely, the method we propose here for the preparation of arrays of magnetic structures is rather simple and it consists in a single step (i.e., the application of stress to generate local deformation).

The material used in the experiments is a commercial AISI 316 austenitic stainless steel. The steel piece was first cut into fine sheets and subsequently polished to mirrorlike appearance. To eliminate possible magnetic contributions created during the initial processing, the sheets were subsequently annealed for 30 min at 1400 K (which is above the reverse, martensite-to-austenite, phase transformation temperature[18]) and cooled to room temperature. Arrays of 15×15 triangular indentations with lateral sizes in the micrometer and submicrometer ranges were prepared by means of a nanoindenter, operating in the load control mode and using a Berkovich-type, pyramidal-shaped, diamond tip. The indentation function consisted of a loading segment of 15 s, applying a maximum forces of 0.75, 2.5, and 9 mN; a load holding segment of 10 s and an unloading segment of 15 s.

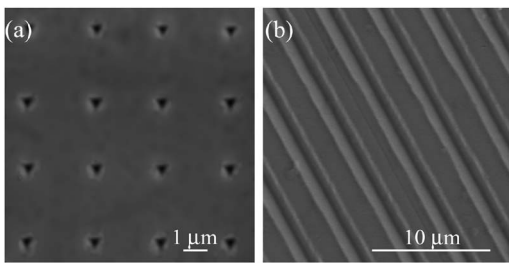a)Electronic mail: jordi.sort@uab.es

FIG. 1. Scanning electron microscopy (SEM) images corresponding to (a) the array of indentations obtained by applying a maximum loading force of 0.75 mN and (b) the array of lines obtained by dragging the nanoindenter tip at 10 μm/s by applying a constant load of 3.5 mN. Note that for the arrays of lines the sample was tilted by 30° during SEM imaging.

Arrays of lines (80 μm long) were prepared by scratching, i.e., dragging the indenter tip at a constant force of 3.5 and 5 mN and at a rate of 10 μm/s. The overall phase composition of the samples was determined by x-ray diffraction. The morphology of the locally deformed regions was examined by scanning electron microscopy (SEM) and atomic force microscopy (AFM). Hysteresis loops of the deformed and undeformed areas were recorded at 6 Hz, using a magneto-optical Kerr effect (MOKE) setup, with a maximum in-plane applied field of 700 Oe. Hysteresis loops were recorded along different in-plane angles to analyze possible effects from magnetic anisotropies. Magnetic force microscopy (MFM) imaging was used to check the local character of the induced ferromagnetism and to probe possible domain patterns within the indented regions.

Shown in Fig. 1(a) is a scanning electron microscopy image of the array of indentations obtained on the steel sheet after applying a maximum loading force of 0.75 mN. The indentations are roughly triangular due to the pyramidal shape of the indenter [as it is also evident from the atomic force microscopy image shown in the upper panel of Fig. 2(a), corresponding to an applied force of 9 mN]. A slight deformation just around each indentation is also observed. For loads of 0.75, 2.5, and 9 mN the lateral dimensions of the indentations are approximately 400 nm, 1 μm, and
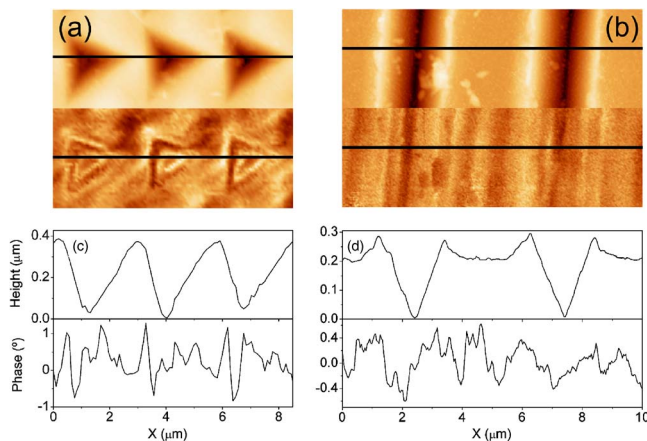

FIG. 2. (Color online) (a) Atomic force microscopy (AFM) image (upper panel) and magnetic force microscopy image (MFM) (bottom panel), corresponding to the array of indentations obtained by applying a maximum load of 9 mN. (b) AFM (upper panel) and MFM (bottom panel) images of a portion of the array of lines obtained by scratching with an applied load of 5 mN. [(c) and (d)] Line profiles from the AFM (i.e., relative height) and MFM (magnetic contrast, i.e., phase) corresponding to the positions indicated in (a) and (b).
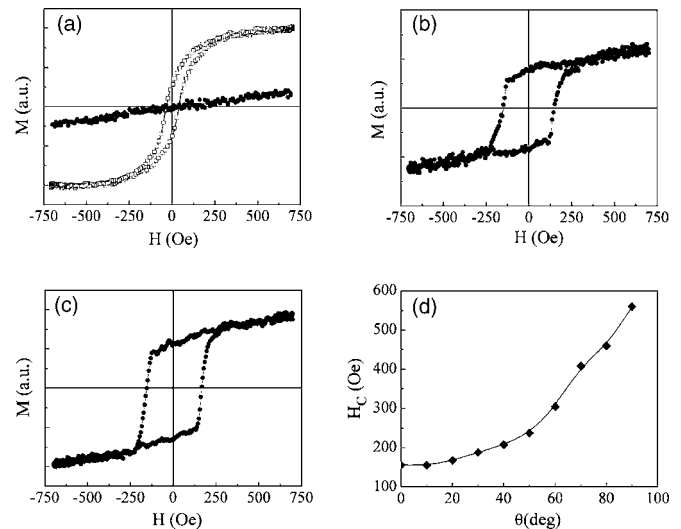

FIG. 3. (a) Hysteresis loop (-□-) obtained after cutting and polishing (before annealing) the austenitic stainless steel, together with the linear relationship (-●-) observed between the magnetization and the applied field after annealing the steel at 1400 K for 30 min. (b) Hysteresis loop corresponding to the array of indentations with lateral size of 1 μm. (c) Hysteresis loop obtained from the array of lines (1.8 μm wide) measured along the direction of the lines. (d) Dependence of the coercivity H_C on the angle of measurement for the array of 1.8 μm wide lines. The lines are guides to the eyes.

2.8 μm, respectively. More complex patterns, e.g., lines, can be easily formed by simply dragging the indenter tip onto the surface of the austenitic steel. Two arrays of lines with widths of 1.8 and 2.3 μm are shown in Fig. 1(b) (SEM) and the upper panel of Fig. 2(b) (AFM), corresponding to applied forces of 3.5 and 5 mN, respectively. It should be noted that to enhance image contrast the sample was tilted by 30° during SEM imaging. The topological profile across the indented lines can be easily seen in the AFM image. Furthermore, from the dependence of the displacement into the sample on the applied force (not shown) an average hardness of 2.7 GPa and a reduced elastic modulus of 220 GPa are obtained, which are values typical for austenitic stainless steel.[19]

Figure 3(a) reveals that when the MOKE measurement is carried out after cutting and polishing the austenitic steel pieces, a clear ferromagnetic hysteresis loop with a coercivity H_C=35 Oe is measured, which indicates that the initial processing (i.e., cutting and polishing) already induces a partial transformation from austenite to martensite. This was confirmed by x-ray diffraction (not shown). The subsequent annealing of the steel at 1400 K completely transforms the martensite back to austenite (as confirmed by x-ray diffraction). Moreover, after annealing, when MOKE measurements are performed away from the arrays of indentations (i.e., undeformed material), a straight line is obtained [see Fig. 3(a)], which is characteristic of a paramagnetic material, as it corresponds to the austenite at room temperature. Note that the MOKE signal represents the change in the angle of polarization of the light as a function of the applied magnetic field and it is proportional to the magnetization of the sample, although quantitative determination of the sample magnetization is not possible by MOKE.

When MOKE measurements are carried out in the indented regions hysteresis loops typical of ferromagnetic behavior are recovered, indicating that nanoindentation is in-

deed a versatile tool to controllably induce ferromagnetism at small length scales in austenitic stainless steel. From the hysteresis loop corresponding to the array of 400 nm [see Fig. 3(b)] a coercivity value $H_C = 150$ Oe is obtained, which represents about a fourfold increase with respect to H_C measured after cutting and polishing the austenitic steel piece (i.e., before annealing). This large H_C may be due to the physical constraints that the reduced sizes of the indented regions impose on the propagation of magnetic domains.[17,20] No variations in H_C are observed when varying the in-plane angle of measurement. Moreover, a linear background is still observed since, although focused down to a few micron spot, the MOKE measurement probes not only the locally deformed (i.e., ferromagnetic) regions but also the paramagnetic surrounding austenite. Similar coercivity values, again without angular dependence, are obtained for the other arrays of triangular indentations. Conversely, for the arrays of lines, the coercivity is found to be dependent on the direction of the measurement. For example, for the array of 1.8 μm wide lines, the coercivity evaluated from the loop recorded along the direction of the lines [Fig. 3(c)] is $H_C = 160$ Oe and it increases progressively as the angle of measurement approaches 90° from the direction of the lines [see Fig. 3(d)], reaching a maximum value of 560 Oe. These results may be interpreted as being due to the competition between magnetostatic energy (which, for the relatively large thickness of the lines, favors magnetization reversal via curling mechanisms or formation of multidomain states) and anisotropy energy.[20–22]

To further assess the local character of the generated ferromagnetism, the indented samples were imaged by MFM. The MFM images, with the corresponding AFM images, of the array of triangular indentations with 2.8 μm lateral size and a portion of lines (2.3 μm wide) are shown in Figs. 2(a) and 2(b), respectively. Dark and bright areas are observed by MFM inside the triangular indentations and a slight contrast is observed in the deformed material surrounding each indentation. As expected, no magnetic contrast was observed in the regions located outside the array of indentations. As can be seen in Fig. 2(b), some fringes can be observed both inside and between the lines (also because the scratch experiments deform, to some extent, the material surrounding the lines). The fact that the MFM images indeed correspond to magnetic (and not simply topological) contrast can be confirmed by plotting line scans across the AFM and MFM images. As shown in Figs. 2(c) and 2(d) the topological (from AFM) and magnetic (from MFM) profiles do not coincide, thus the MFM images are indeed representative of the multidomain structure inside the indentations. Nevertheless, these images are not straightforward to interpret because the surfaces are not flat and, therefore, both in-plane and out-of-plane magnetization components probably coexist. However, MFM clearly confirms that ferromagnetism is locally induced by the nanoindentation experiments.

The indented austenitic steel sheet was finally annealed again at 1400 K. This process resulted in a MOKE signal without hysteresis, resembling the straight line shown in Fig.

3(a). Namely, the magnetic information was erased.

The process of *selectively* and *locally* inducing ferromagnetism in a nonmagnetic stainless steel could, in principle, be also performed by means of other deformation techniques, such as friction experiments or by imprinting, in parallel, a previously designed mold. Hence, this microstructuration technique could have a varied range of applications, including recording media or magnetic sensors.

In summary, we demonstrate that by means of nanoindentation experiments it is possible to fabricate, in a controlled manner, periodic arrays of micrometric and submicrometric magnetic structures at the surface of nonmagnetic stainless steel. This method is based on the mechanically induced martensitic phase transformation that occurs in austenitic steel. The induced ferromagnetism can be erased by subsequently subjecting the locally deformed sheets to annealing processes at temperatures high enough to transform the martensite back to austenite.

[1]S. L. Chawla and R. K. Gupta, *Materials Selection for Corrosion Control* (ASM International, Materials Park, OH, 1997), Chap. 10.
[2]H. Mughrabi and H. J. Christ, ISIJ Int. **37**, 1154 (1997).
[3]S. S. Hecker, M. G. Stout, K. P. Staudhammer, and J. L. Smith, Metall. Trans. A **13**, 619 (1982).
[4]E. Nagy, V. Mertinger, F. Tranta, and J. Sólyom, Mater. Sci. Eng., A **378**, 308 (2004).
[5]D. L. Bourell, Acta Metall. **31**, 609 (1983).
[6]S. M. Bruemmer and G. S. Was, J. Nucl. Mater. **216**, 348 (1994).
[7]J. Ding, H. Huang, P. G. McCormick, and R. Street, J. Magn. Magn. Mater. **139**, 109 (1995).
[8]I. Mészáros and J. Prohászka, J. Mater. Process. Technol. **161**, 162 (2005).
[9]A. Miller, Y. Estrin, and X. Z. Hu, Scr. Mater. **47**, 441 (2002).
[10]S. S. M. Tavares, H. F. G. Abreu, J. M. Neto, M. R. da Silva, and I. Popa, J. Alloys Compd. **358**, 152 (2003).
[11]L. Zhang, Y. Kamada, H. Kikuchi, K. Mumtaz, K. Ara, S. Takahashi, M. Sato, and T. Tsukada, J. Magn. Magn. Mater. **271**, 402 (2004).
[12]H. Ishigaki, Y. Konishi, K. Kondo, and K. Koterazawa, J. Magn. Magn. Mater. **193**, 466 (1999).
[13]Y. Nagae, Mater. Sci. Eng., A **387-389**, 665 (2004).
[14]K. Mumtaz, S. Takahashi, J. Echigoya, Y. Kamada, L. F. Zhang, H. Kikuchi, K. Ara, and M. Sato, J. Mater. Sci. **39**, 85 (2004).
[15]M. Kuroda, S. Yamanaka, and Y. Isobe, NDT & E Int. **38**, 53 (2005).
[16]Z. Ni, X. Wang, E. Wu, and G. Liu, J. Appl. Phys. **98**, 114319 (2005).
[17]J. I. Martín, J. Nogués, K. Liu, J. L. Vicent, and I. K. Schuller, J. Magn. Magn. Mater. **256**, 449 (2003).
[18]K. Mumtaz, S. Takahashi, J. Echigoya, Y. Kamada, L. F. Zhang, H. Kikuchi, K. Ara, and M. Sato, J. Mater. Sci. **39**, 1997 (2004).
[19]A. Rodrigo and H. Ichimura, Surf. Coat. Technol. **148**, 8 (2001).
[20]R. Skomski, J. Phys.: Condens. Matter **15**, R841 (2003).
[21]W. Wernsdorfer, B. Doudin, D. Mailly, K. Hasselbach, A. Benoit, J. Meier, J.-Ph. Ansermet, and B. Barbara, Phys. Rev. Lett. **77**, 1873 (1996).
[22]J. Qin, J. Nogués, M. Mikhaylova, A. Roig, J. S. Muñoz, and M. Muhammed, Chem. Mater. **17**, 1829 (2005).